IASS 2020/21 SURREY 7
International Conference on Spatial Structures 2020/21

Proceedings of the IASS Annual Symposium 2020/21 and the 7th International Conference on Spatial Structures
Inspiring the Next Generation
23 – 27 August 2021, Guilford, UK
S.A. Behnejad, G.A.R. Parke and O.A. Samavati (eds.)

Developing a polyhedral graphic statics formulation for tetrahedral truss analysis

Salma MOZAFFARI[*,a], Márton HABLICSEK[b], Masoud AKBARZADEH[c], Thomas VOGEL[a]

[*,a] Institute of Structural Engineering, ETH Zurich
Stefano-Franscini-Platz 5, HIL E 34.2, 8093 Zurich, Switzerland
mozaffari@ibk.baug.ethz.ch

[b] Mathematical Institute, Leiden University

[c] Polyhedral Structures Laboratory, School of Design, University of Pennsylvania, Philadelphia, USA

Abstract
This paper presents procedures to generate tetrahedral truss topologies as an input form for polyhedral graphic statics and develops an algebraic formulation to construct their force diagrams. The recent algebraic 3D graphic statics constructs reciprocal polyhedral diagrams with either form or force as input. However, the input is usually a set of polyhedrons or self-stressed networks. Another implementation of polyhedral graphic statics includes general truss topologies. Nevertheless, the starting geometry is usually the global force diagram and based on its modification or subdivision, a form is constructed. Therefore, currently, there exists no formulation to analyze a spatial truss using polyhedral graphic statics. This paper develops an algorithm to build upon the algebraic 3D graphic statics formulation to construct the force diagram and analyze spatial trusses that are not self-stressed structures. The article also shows how the proper definition of the external spaces between the applied loads and reaction forces and the tetrahedral subdivision of the truss make it possible to construct the reciprocal force diagram.

Keywords: 3D graphic statics, reciprocal polyhedral diagrams, algebraic formulation, space truss.

1. Introduction
The *polyhedral graphic statics* is based on Maxwell's principles of reciprocal diagrams and Rankin's extension to polyhedral reciprocals [1–3]. As opposed to *vector-based 3D graphic statics* [4–7], the form and force diagrams are fully reciprocal polyhedrons, and a closed force polyhedron demonstrates the equilibrium at each node. The area and the normal vector of faces in the force polyhedron determine the force magnitude and force type of its reciprocal member in the form diagram. Akbarzadeh et al. have clarified and illustrated Rankin's propositions of polyhedral reciprocal diagrams [8, 9]. Although the contribution is relatively recent, it has shown potentials for form-finding and design of spatial structures [10–14]. Also, a handful of computational techniques exists to generate the dual diagram, provide algorithms for manipulation of form and force polyhedrons, and create force visualizations by geometrical summations of the dual diagrams [9, 15–22].

1.1. Problem statement and objectives
Limitations exist regarding the type of input geometries the computational methods of polyhedral graphic statics can handle; the *algebraic 3D graphic statics* constructs the dual polyhedral diagram with either form or force as input [19, 20]. However, the input is usually a set of closed polyhedrons or a self-stressed network. Similarly, the examples for constructing dual diagrams using projective geometry and

Airy stress functions have also been restricted to self-stressed topologies [17, 23]. More general spatial truss typologies, with vertical loads and reaction forces, are covered in [11, 24]. Nevertheless, the input geometry is usually the global force diagram and based on its modification or subdivision, a form is constructed. Furthermore, the *PolyFrame* and *3D Graphic Statics* plugins for *Rhino* and *Grasshopper* only work with compression- or tension-only structures [21, 22]. Therefore, currently, there exists no formulation to analyze a spatial truss with both compression and tension members using polyhedral graphic statics.

This paper intends to develop an algebraic formulation to analyze spatial truss systems using polyhedral graphic statics. The algorithm builds upon the algebraic 3D graphic statics [19] to construct the force diagram for tetrahedral geometries that are not self-stressed structures. The article shows how creating a proper datastructure (using the correct definition of the external spaces between the applied loads and reaction forces and the tetrahedral subdivision of the truss) makes it possible to analyze the truss and construct the reciprocal force diagram. The study's ultimate goal is to extend the authors' previous research in 2D [25, 26] to generate 3D strut-and-tie models and stress fields for reinforced concrete design.

2. Methodology

As mentioned, the algebraic implementation of polyhedral graphic statics [19] can construct the dual diagram, given an input primal (form or force) diagram. However, the input truss topology should be a closed or a self-stressed network, and this is not practical for the analysis of most spatial trusses. This section provides the steps for constructing the force diagram for a tetrahedral truss and explains how the algebraic equations help calculate edge lengths of the force diagram. To clarify the procedure of constructing the force diagram for a spatial truss, we first explain the notation used in 2D graphic statics, then extend it to the 3D version.

2.1. Notation and reciprocity in 2D graphic statics

Fig.1 shows an example of a simple 2D truss (form diagram) with vertices 0-5, faces *A*-*C* (i.e., the 2D subspace assignments), and edges $(0,1)$, $(1,2)$, etc. The open external faces are shown with dashed lines. The internal vertices 1-3, edges and faces of the form are respectively reciprocal to the faces 1-3, edges, and vertices *A*-*C* of the force diagram. The closed polygons in the force diagram show the external and nodal equilibrium of forces (Fig.1c). To construct the force diagram, first, the global force polygon showing the external equilibrium is made by looping the external faces *A*-*B*-*C*-*A* and drawing the vectors parallel to vectors (0,1), (5,3) and (4,2) that separate these faces (Fig.1c-left). The length of vector *AB* in the force diagram is proportional to the applied load, and the magnitude of the support reactions and truss member forces will be defined based on this proportion after the completion of the force diagram. Once the topology of the global force polygon is known, the rest of the force polygons for each nodal equilibrium can be drawn by traversing the faces surrounding each vertex in the form and drawing lines parallel to edges shared between these faces until a closed polygon is formed. For example, for vertex 1 in Fig.1a, looping faces *A*-*B*-*D*-*A* around node 1 leads to construction of polygon *ABD* in Fig.1c. The process continues for all other internal vertices till the force diagram is completed (Fig.1b). The edge vectors in each force polygon assure a closed loop, and the sharing edge vectors between two neighboring faces always have opposite directions. The type of forces can be defined using the edge vectors [27]. For example, assume vertex 1 and edge $(2,1)$ in Fig.1a and their corresponding polygon 1 and edge *DA* in Fig.1c, the vector *DA* goes from D to A and this is towards vertex 1, so edge $(1,2)$ is in compression.

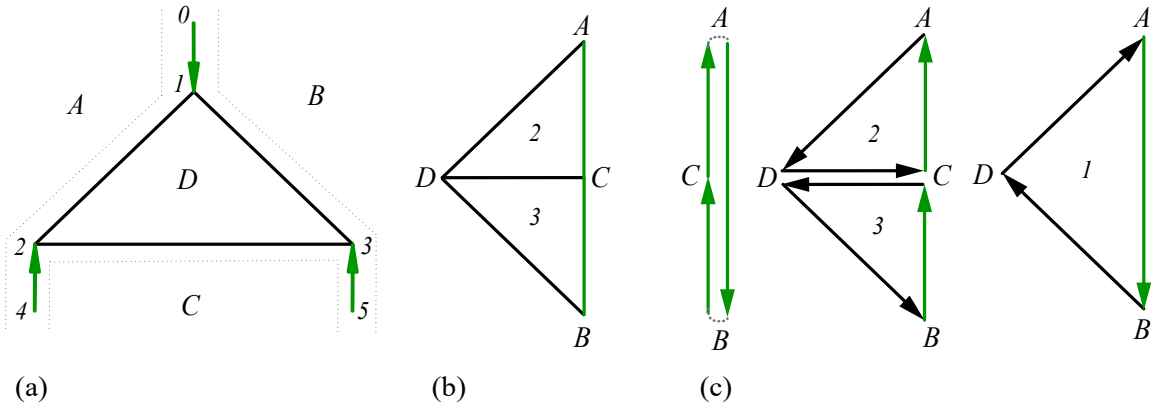

Figure 1: (a) 2D truss (form diagram); (b) 2D force diagram; (c) global force polygon (left), nodal force polygons (middle and right).

2.2. Polyhedral graphic statics for tetrahedral trusses

The notation in polyhedral graphic statics can be seen as an extension of the 2D notation. The 3D subspace assignments (i.e., cells) are defined through faces as opposed to the edges in 2D. Fig.2a-c shows an example of a spatial truss (form diagram) with vertices 0-7, faces, cells *A*-*E*, and edges $(0,1)$, $(1,2)$, etc. The internal vertices 1-4, edges, faces, and cells in the form diagram are respectively reciprocal to the cells 1-4, faces, edges, and vertices *A*-*E* of the force diagram (Fig.2a and f). In polyhedral graphic statics, the faces are required to be planar. The tetrahedral truss typologies of this paper, following a triangulation rule, assure the stability of the form and the planarity requirement of faces between the truss members. The closed polyhedrons in the force diagram show the nodal equilibrium of forces at each truss internal vertex (Fig.2f). Each edge in the form is parallel to its reciprocal face normal in the force and vice versa. The area of the faces in the force diagram equals the magnitude of the forces in the truss members.

2.2.1. Construction of polyhedral force diagram

The steps of constructing the polyhedral force diagram, given a spatial truss in Fig.2a is clarified as follows: (i) Define faces and cells: in 2D, the faces are assigned based on the edges that separate them; in 3D, the cells are created after the faces are appropriately defined (Fig.2b and c). The faces should be planar, and the neighboring faces share one edge. The defined cells should not intersect, and neighboring cells share one face.

(ii) Construct the load face: like 2D, the first step is to construct the global force polyhedron showing the external equilibrium. For that, the face reciprocal to the load edge $(0,1)$ is created first. The topology of the load face *ABC* is discovered by traversing cells *A*-*B*-*C*-*A* around edge $(0,1)$ and drawing the normal vector of the faces separating these cells (Fig.2d). The normal vectors with proper lengths (the area of the face is proportional to the load magnitude) form a closed face *ABC*, and this face is perpendicular to the load edge $(0,1)$. The edge vectors of the face define the face cycle, and the direction of the face normal $\mathbf{n}_{(0,1)}$ is assigned based on the right-hand rule. The direction of the face normal, and therefore the face cycle should agree with the load direction.

(iii) Construct the global force polyhedron: the faces reciprocal to reaction edges $(2,5)$, $(3,6)$, and $(4,7)$ can be created similarly. Since the reactions are unknown, their directions can be discovered using the known edge vectors of the load face (Fig.2e-top). For example, face *ACE* reciprocal to reaction $(2,5)$ shares edge *AC* with the load face *ABC*. Edge *AC* in *ACE* should have an opposite direction. The other

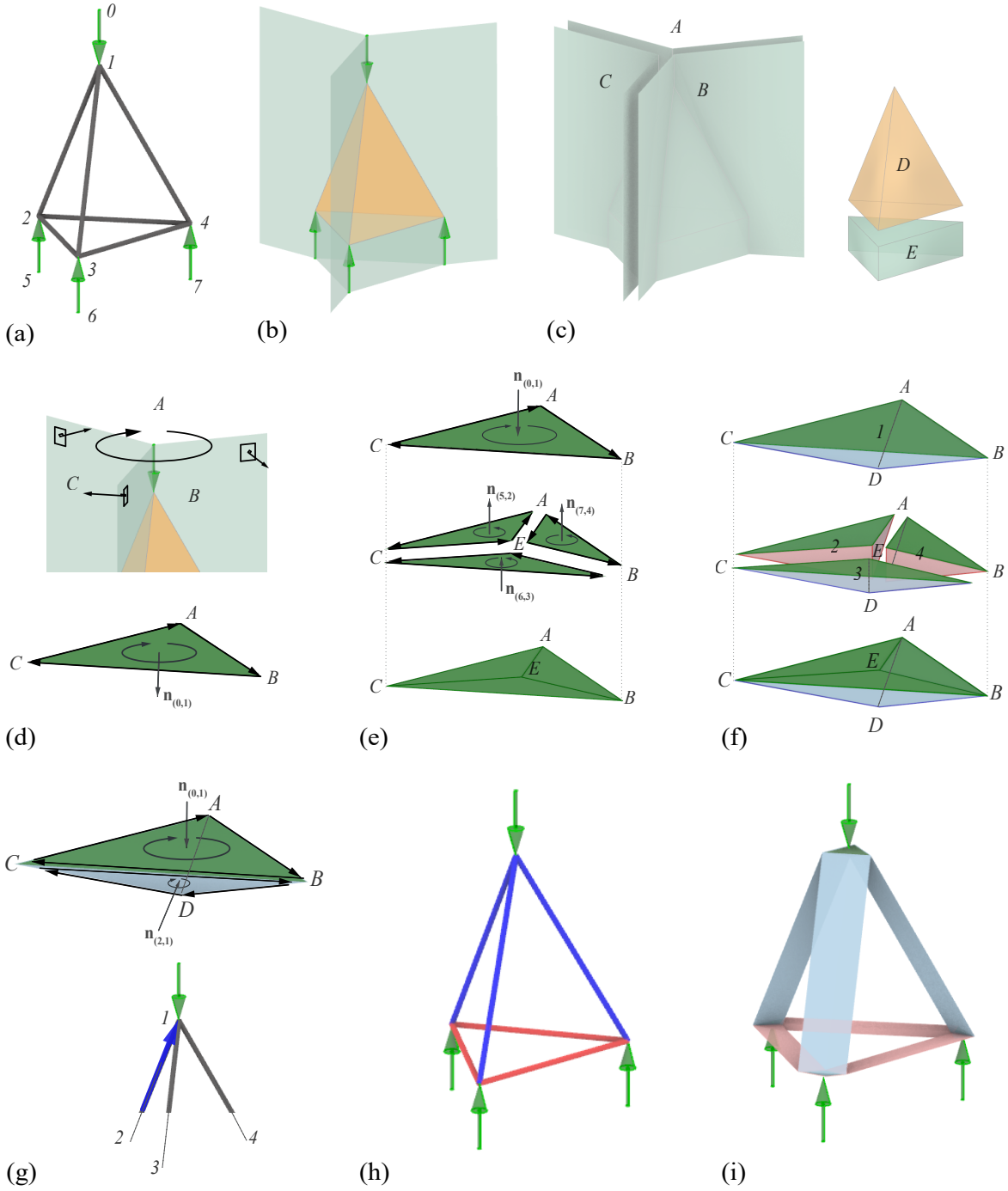

Figure 2: (a) Space truss (form diagram); (b) face definition; (c) assigned external and internal cells; (d) constructing the load face; (e) constructing the global force polyhedron; (f) force polyhedrons showing equilibrium at nodes 1-4 and the completed force diagram; (g) defining the force type for edge (2,1); (h) force types (blue:compression, red:tension); (i) force visualization.

edge vectors of this face (i.e., *CE* and *EA*) are defined based on the direction of *AC* to form a closed polygon (Fig.2 e-middle). Based on the cycle and normal $\mathbf{n}_{(5,2)}$ of face *ACE*, the direction of the reaction force is defined. The reaction force magnitude is proportional to the area of face *ACE*. The two other load faces can be constructed similarly. Eventually, the four faces (*ABC*, *ACE*, and *AEB*, and *BEC*) form

a flat global force polyhedron shown in Fig.2e-bottom.

(iv) Construct the complete force diagram: the same procedure is applied to the remaining edges of the form to construct the rest of the force diagram's faces. Ultimately, for each nodal equilibrium (at vertices 1-4) a force polyhedron (i.e., a cell) is produced, and the force diagram is completed (Fig.2f). The truss member forces will be proportional to the face areas in the force polyhedrons.

(v) Define the type of forces: to determine if the truss member forces are in compression or tension, the cycle of faces in each force polyhedron should be specified. For example, the force polyhedron related to equilibrium at vertex 1 in Fig.2g, shares face *ABC* with the global force polyhedron, and the face cycle should be preserved. Now that edge vectors in *ABC* are known, cycles of its neighboring faces *CBD*, *BAD*, and *ACD* can be specified. As an example, face *CBD* shares edge *BC* with face *ABC*, but their vectors should be opposite. Based on this flipped vector, the cycle of face *CBD* can be defined. Face *CBD* is reciprocal to edge $(1,2)$ and it is in compression since the normal $\mathbf{n}_{(1,2)}$ is towards node 1. The cycles of other faces in cell 1 and the type of forces for the rest of the members at node 1 can be specified similarly.

(vi) Force visualization: the proportional magnitude of forces in each truss member can be illustrated by the geometrical summation of the form diagram and a down-scaled force diagram using the *Minkowski sum* [15, 24, 25].

2.2.2. Algebraic implementation

The explained procedure is implemented in a computational setup with algebraic equations to calculate the dual edge lengths and construct the force diagram. After defining the truss geometry and faces, the datastructure is built using PolyFrame [21]. The load faces are constructed using algebraic equations for 2D polygons. Since the load faces are closed polygons, sum of the edge vectors of each load face has to be the zero vector. Thus, each load face provides a vector equation:

$$\sum_{e_j} \mathbf{u}_j q_j = \mathbf{0} \tag{1}$$

where e_j are the edges of the load face, $\mathbf{u}_j$ are their direction vectors, and q_j are the variables representing the edge lengths for e_j. These equations can be written for every load face, and the topology of the load faces can be described through a $[2f_l \times e_l]$ matrix $\mathbf{A}_l$, with f_l the number of load faces in the force diagram, and e_l the total number edges for the load faces [28, 29]:

$$\mathbf{A}_l \mathbf{q}_l = \mathbf{0} \tag{2}$$

where $\mathbf{q}_l$ is the $[e_l \times 1]$ vector of edge lengths for the load faces. The solutions of Eq.2 can be obtained using the *Moore-Penrose Inverse* (MPI) $\mathbf{A}_l^+$ of $\mathbf{A}_l$ [30, 31]:

$$\mathbf{q}_l = (\mathbf{I} - \mathbf{A}_l^+ \mathbf{A}_l)\xi \tag{3}$$

where $\mathbf{A}_l^+$ is a $[e_l \times 2f_l]$ matrix, $\mathbf{I}$ is the $[e_l \times e_l]$ identity matrix, and ξ is any $[e_l \times 1]$ vector. We choose ξ to be the $[e_l \times 1]$ vector of ones to achieve $\mathbf{q}_l$ with well-distributed edge lengths [19, 32]. As clarified in the previous section, as soon as the load face is known, the topology and cycles of reaction and other faces can be specified, so the edge lengths for the rest of the force diagram can be calculated. Similar formalism can be applied in constructing the complete force diagram in three-dimensional space [19]. The topology of the force diagram with f faces and e edges can be described by a $[3f \times e]$ matrix $\mathbf{A}$, and Eq.4 imposes the condition of closed face polygons in the three-dimensional space:

$$\mathbf{A}\mathbf{q} = \mathbf{0} \tag{4}$$

where $\mathbf{q}$ is the $[e \times 1]$ vector of all edge lengths. The calculated edge lengths for the load faces from Eq.3 impose extra constraints. Each load face edge e_i with a predefined length q_i provides a vector equation:

$$\mathbf{l}_i^T \mathbf{q} = q_i \tag{5}$$

where $\mathbf{l}_i$ is the $[e \times 1]$ column vector whose entries are all zero except at the index of e_i where it is one. Together with Eq.4, we obtain a linear equation system describing the topology of the force diagram with predefined edge lengths for the load faces:

$$\mathbf{B}\mathbf{q} = \mathbf{b} \tag{6}$$

where matrix $\mathbf{B}$ is obtained by stacking matrix $\mathbf{A}$ and row vectors $\mathbf{l}_i^T$, and vector $\mathbf{b}$ is obtained by stacking a zero vector with the known edge lengths q_i [20, 26]. The solutions of Eq.6 can be described as:

$$\mathbf{q} = \mathbf{B}^+\mathbf{b} + (\mathbf{I} - \mathbf{B}^+\mathbf{B})\omega \tag{7}$$

where $\mathbf{B}^+$ is the MPI of $\mathbf{B}$, $\mathbf{I}$ is the $[e \times e]$ identity matrix, and ω is any $[e \times 1]$ vector. Again, we choose ω to be a vector of ones to obtain a solution $\mathbf{q}$ with well-distributed entries. After solving for $\mathbf{q}$, which includes all the edge lengths, the force diagram can be constructed using a *graph search method* explained in [19]. The magnitude and type of forces can then be discovered.

3. Examples

The force diagram, force types, and force visualization for the examples of this section are calculated with the computational implementation explained in the previous section. The examples here are limited to tetrahedral truss geometries with vertical loads and reactions. Also, the trusses do not have any internal nodes, i.e., there is either a load or support at each node. Moreover, the loads do not cantilever outside the space surrounded by reactions' line of actions (this avoids having complications in making the load faces or having self-intersecting faces in the force diagram, which is out of the scope of this paper).

Fig.3a shows a tetrahedral truss with four supports. To keep the faces triangulated and the form stable, a diagonal truss member is added to the bottom face between the supports. As a result, two internal orange cells are created in Fig.3c. By increasing the number of loads and supports, more options exist for triangulation of the form. Some options for the case of two loads and four supports are shown in Fig.4. It should be noted that the configuration of the three diagonal members in Fig.4d results in a single internal cell. The external symmetry between loads and supports in Fig.4a-d results in zero areas and therefore zero forces in the diagonal members, as the solution for Fig.4a illustrates in Fig.5. The diagonal members act as bracing to stabilize the form, but do not participate in the equilibrium of the forces.

The force diagram can also be generated for non-symmetrical scenarios with several loads and supports, as long as the faces are kept planar. In the example of Fig.6, to assure planarity, each load should be connected to at least three supports. One application of force visualization (i.e., Minkowski sum of form and force diagrams) in Fig.6e can be the depiction of discontinuous stress fields for a block of continuous material like reinforced concrete if the generated form is considered a 3D strut-and-tie model [15, 26].

4. Conclusion and outlook

The paper shows that the algebraic formulation of polyhedral graphic statics can be utilized to analyze spatial trusses. The step-by-step procedure for constructing the polyhedral force diagram is explained, and the algebraic equations for calculating the edge lengths of the force diagram are provided. Although the input geometries can include typologies that are not self-stressed, the current computational implementation is restricted to specific geometries; the input truss has a tetrahedral shape to avoid non-planar faces. The truss does not have any internal nodes, i.e., there is either a load or support at each node.

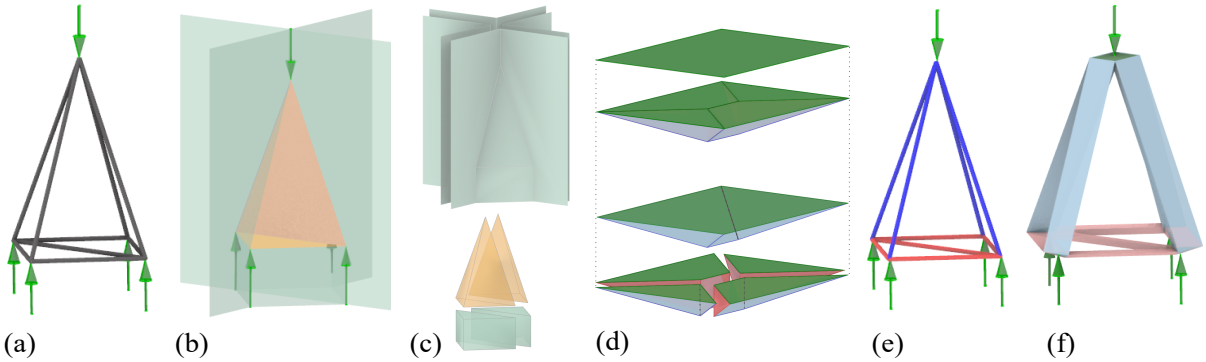

Figure 3: (a) Space truss (form diagram); (b) face definition; (c) assigned external and internal cells; (d) load face, complete force diagram, and nodal force polyhedrons; (e) force types (blue:compression, red:tension); (f) force visualization.

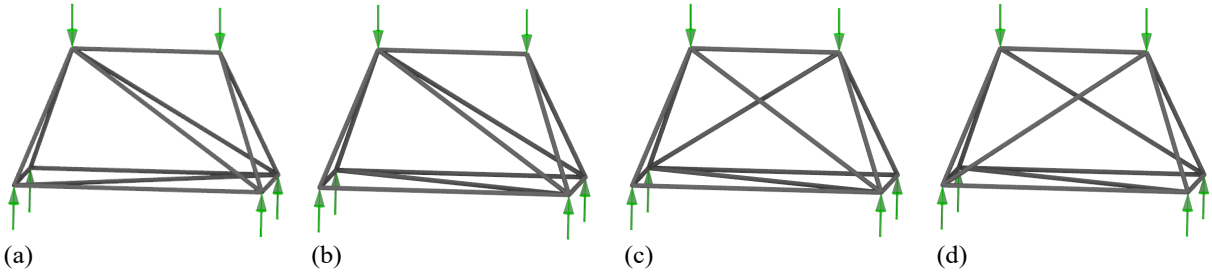

Figure 4: Triangulation solutions for the case of two loads and four supports.

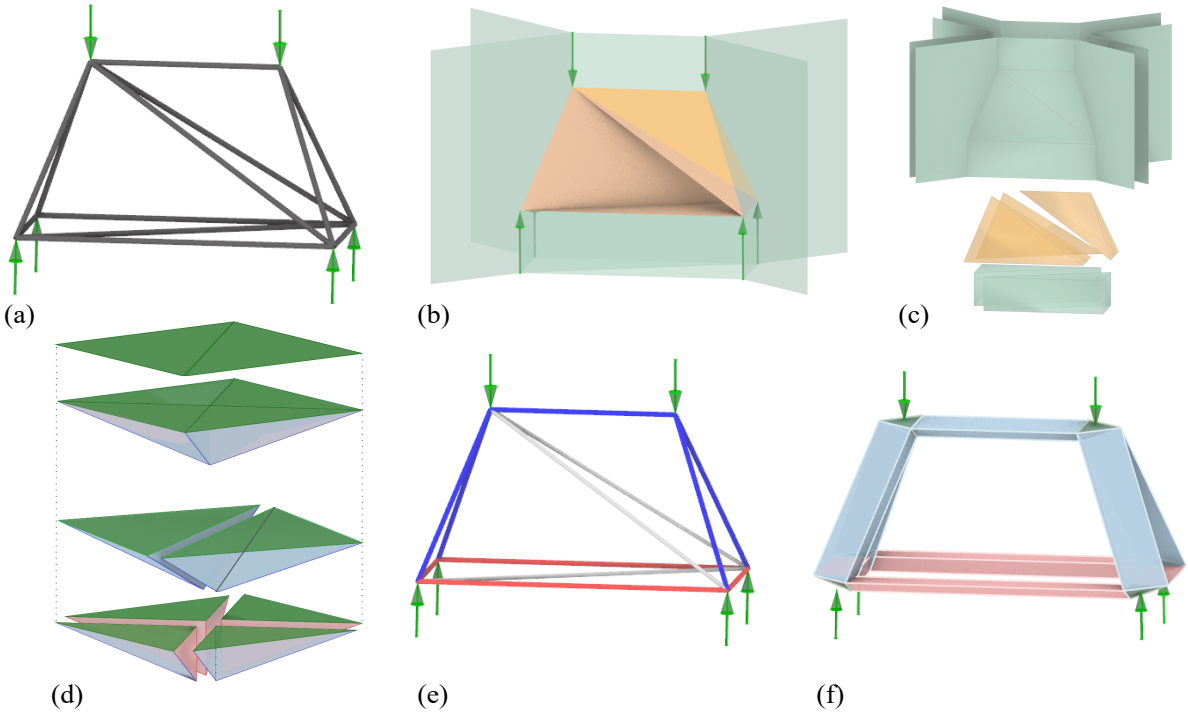

Figure 5: (a) Space truss (form diagram); (b) face definition; (c) assigned external and internal cells; (d) load faces, complete force diagram, and nodal force polyhedrons; (e) force types (blue:compression, red:tension); (f) force visualization.

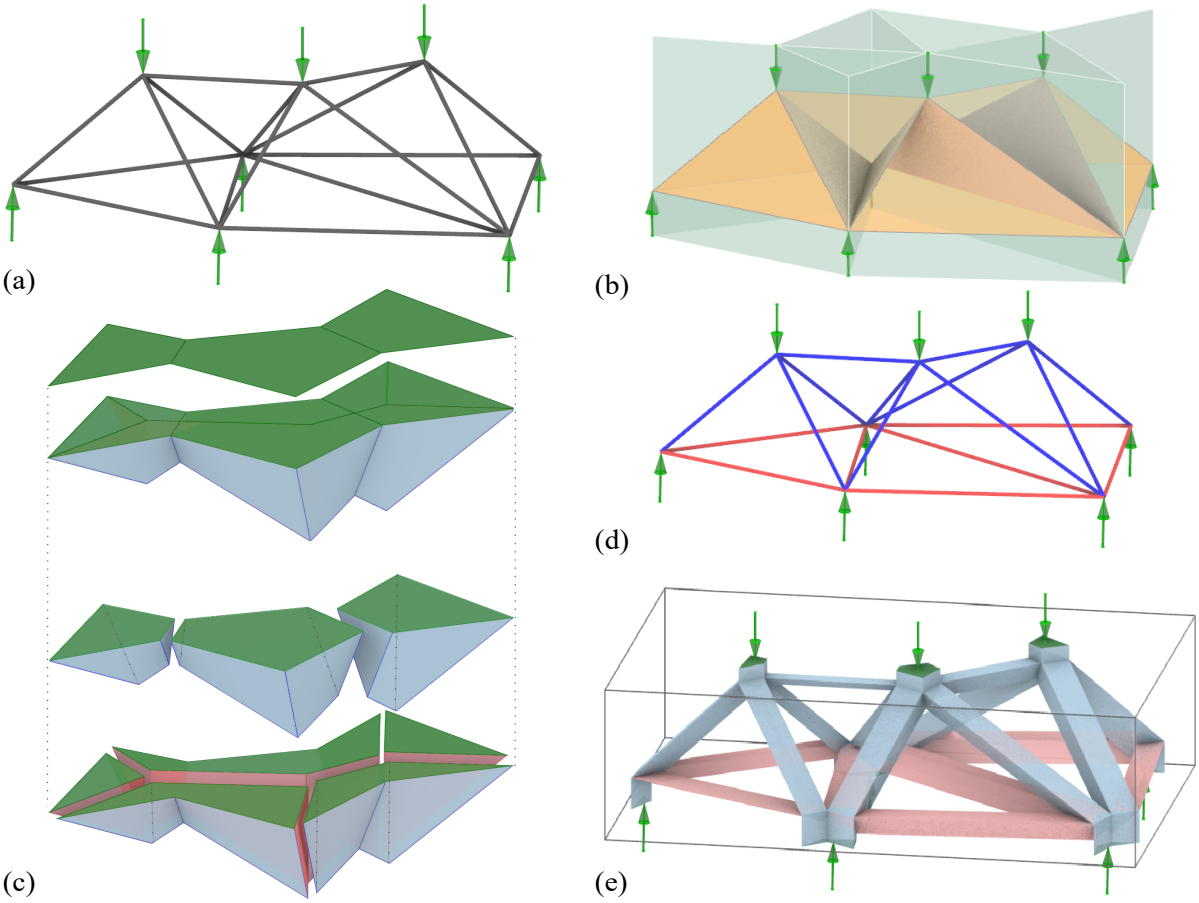

Figure 6: (a) Space truss (form diagram); (b) face definition; (c) load faces, complete force diagram, and nodal force polyhedrons; (d) force types (blue:compression, red:tension); (e) discontinuous stress fields for a reinforced concrete block.

Moreover, this article does not include examples with cantilever loads or reaction forces and loads of various angles.

As the ultimate goal of this study is to generate strut-and-tie models and stress fields for design and analysis of reinforced concrete elements, the future work is focused on the following: (i) automatic generation of the tetrahedral trusses accounting for the concrete design domain and locations of external loads and supports, (ii) adjusting the areas of the load faces in accordance to the magnitudes of the applied loads, and (iii) modification of the initial geometries by increasing the resolution (i.e., adding internal nodes or members).

References

[1] J. Maxwell, "On reciprocal figures and diagrams of forces," *Philosophical Magazine Series 4*, vol. 27, no. 182, pp. 250–261, 1864.

[2] W. Rankine, "Principle of the Equilibrium of Polyhedral Frames," *Philosophical Magazine Series 4*, vol. 27, no. 180, p. 92, 1864.

[3] J. Maxwell, "On reciprocal figures, frames, and diagrams of forces," *Earth and Environmental Science Transactions of the Royal Society of Edinburgh*, vol. 26, no. 1, pp. 1–40, 1870.

[4] L. Cremona, *Graphical statics: two treatises on the graphical calculus and reciprocal figures in graphical statics.* Oxford: Clarendon Press, 1890.

[5] M. Schrems and T. Kotnik, "On the extension of graphical statics into the 3rd dimension," in *Proceedings of the Second International Conference on Structures and Architecture*, 2013.

[6] J. Jasienski, P. D'Acunto, P. Ohlbrock, and C. Fivet, "Vector-based 3d graphic statics (part ii): construction of force diagrams," in *Proceedings of IASS Annual Symposia*, International Association for Shell and Spatial Structures (IASS), 2016.

[7] P. D'Acunto, J. Jasienski, P. Ohlbrock, C. Fivet, J. Schwartz, and D. Zastavni, "Vector-based 3d graphic statics: A framework for the design of spatial structures based on the relation between form and forces," *International Journal of Solids and Structures*, vol. 167, pp. 58–70, 2019.

[8] M. Akbarzadeh, T. Van Mele, and P. Block, "3D Graphic Statics: Geometric Construction of Global Equilibrium," in *Proceedings of the International Association for Shell and Spatial Structures (IASS) Symposium*, 2015.

[9] M. Akbarzadeh, T. Van Mele, and P. Block, "On the equilibrium of funicular polyhedral frames and convex polyhedral force diagrams," *Computer-Aided Design*, vol. 63, pp. 118–128, 2015.

[10] M. Bolhassani, M. Akbarzadeh, M. Mahnia, and R. Taherian, "On structural behavior of a funicular concrete polyhedral frame designed by 3d graphic statics," in *Structures*, vol. 14, pp. 56–68, Elsevier, 2018.

[11] J. Lee, T. Van Mele, and P. Block, "Form-finding explorations through geometric transformations and modifications of force polyhedrons," in *Proceedings of the International Association for Shell and Spatial Structures (IASS) Symposium*, (Tokyo, Japan), 2016.

[12] M. Akbarzadeh, T. Van Mele, and P. Block, "Three-dimensional compression form finding through subdivision," in *"Proceedings of the International Association for Shell and Spatial Structures (IASS) Symposium"*, vol. 21, pp. 1–7, 2015.

[13] F. Heisel, J. Lee, K. Schlesier, M. Rippmann, N. Saeidi, A. Javadian, A. Nugroho, T. Van Mele, P. Block, and D. Hebel, "Design, cultivation and application of load-bearing mycelium components," *International Journal of Sustainable Energy Development*, vol. 6, no. 1, pp. 296–303, 2017.

[14] M. Akbarzadeh, M. Bolhassani, A. Nejur, J. Yost, C. Byrnes, J. Schneider, U. Knaack, and C. Costanzi, "The design of an ultra-transparent funicular glass structure," in *Structures Congress 2019: Blast, Impact Loading, and Research and Education*, pp. 405–413, American Society of Civil Engineers Reston, VA, 2019.

[15] A. McRobie, "Maxwell and Rankine reciprocal diagrams via Minkowski sums for two-dimensional and three-dimensional trusses under load," *International Journal of Space Structures*, vol. 31, no. 2-4, pp. 203–216, 2016.

[16] J. Lee, *Computational design framework for 3D Graphic Statics*. PhD thesis, ETH Zurich, Department of Architecture, Zurich, 2018.

[17] M. Konstantatou, P. D'Acunto, and A. McRobie, "Polarities in structural analysis and design: n-dimensional graphic statics and structural transformations," *International Journal of Solids and Structures*, vol. 152, pp. 272–293, 2018.

[18] M. Konstantatou, P. D'Acunto, A. McRobie, and J. Schwartz, "Unified geometrical framework for the plastic design of reinforced concrete structures," *Structural Concrete*, 2020.

[19] M. Hablicsek, M. Akbarzadeh, and Y. Guo, "Algebraic 3d graphic statics: Reciprocal constructions," *Computer-Aided Design*, vol. 108, pp. 30–41, 2019.

[20] M. Akbarzadeh and M. Hablicsek, "Algebraic 3d graphic statics: Constrained areas," *arXiv preprint arXiv:2007.15133*, 2020.

[21] A. Nejur and M. Akbarzadeh, "Polyframe, efficient computation for 3d graphic statics," *Computer-Aided Design*, vol. 134, p. 103003, 2021.

[22] O. Graovac, "3D Graphic Statics: a structural form-finding plugin for generating compression-only funicular structures.." https://www.food4rhino.com/app/3d-graphic-statics, 2021.

[23] A. McRobie, W. Baker, T. Mitchell, and M. Konstantatou, "Mechanisms and states of self-stress of planar trusses using graphic statics, part ii: Applications and extensions," *International Journal of Space Structures*, vol. 31, no. 2-4, pp. 102–111, 2016.

[24] J. Lee, T. Van Mele, and P. Block, "Disjointed force polyhedra," *Computer-Aided Design*, vol. 99, pp. 11–28, 2018.

[25] S. Mozaffari, M. Akbarzadeh, and T. Vogel, "Generation of strut-and-tie models and stress fields for structural concrete," in *Structures Congress 2019: Blast, Impact Loading, and Research and Education*, pp. 353–361, 2019.

[26] S. Mozaffari, M. Akbarzadeh, and T. Vogel, "Graphic statics in a continuum: Strut-and-tie models for reinforced concrete," *Computers & Structures*, vol. 240, p. 106335, 2020.

[27] E. Allen and W. Zalewski, *Form and forces: designing efficient, expressive structures*. John Wiley & Sons, 2009.

[28] T. Van Mele and P. Block, "Algebraic graph statics," *Computer-Aided Design*, vol. 53, pp. 104–116, 2014.

[29] V. Alic and D. Åkesson, "Bi-directional algebraic graphic statics," *Computer-Aided Design*, vol. 93, pp. 26–37, 2017.

[30] E. Moore, "On the reciprocal of the general algebraic matrix," *Bulletin of American Mathematical Society*, vol. 26, pp. 394–395, 1920.

[31] R. Penrose, "A generalized inverse for matrices," in *Mathematical proceedings of the Cambridge philosophical society*, vol. 51(3), pp. 406–413, Cambridge University Press, 1955.

[32] M. Akbarzadeh and M. Hablicsek, "Geometric degrees of freedom and non-conventional spatial structural forms," in *Design Modelling Symposium Berlin*, pp. 3–17, Springer, 2019.